Information depths of analytical techniques assessing whitefish otolith chemistry

Lill, Jan-Olof; Finnäs, Viktor; Heimbrand, Y.; Blass, M.; Fröjdö, Sören; Lahaye, Y.; Slotte, Joakim; Nyman, Johan; Jokikokko, E.; von Numers, M.; Hägerstrand, Henry

Published in:
Nuclear Instruments and Methods in Physics Research Section B: Beam Interactions with Materials and Atoms

DOI:
10.1016/j.nimb.2019.07.033

Published: 15/08/2020

Document Version
Accepted author manuscript

Document License
CC BY-NC-ND

Information depths of analytical techniques assessing whitefish otolith chemistry

J-O. Lill[a], V. Finnäs[b], Y. Heimbrand[c], M. Blass[c], S. Fröjdö[d], Y. Lahaye[e], J.M.K. Slotte[f], J. Nyman[g], E. Jokikokko[h] M. von Numers[b], H. Hägerstrand[b,i]

[a]Accelerator Laboratory, Turku PET Centre, Åbo Akademi University, Finland
[b]Environmental and Marine Biology, Faculty of Science and Engineering, Åbo Akademi University, Finland
[c]Institute of Coastal Research, Department of Aquatic Resources, Swedish University of Agricultural Sciences, Sweden
[d]Geology, Faculty of Science and Engineering, Åbo Akademi University, Finland
[e]Finnish Isotope Geosciences Laboratory, Geological Survey of Finland, Finland
[f]Physics, Faculty of Science and Engineering, Åbo Akademi University, Finland
[g]Pharmacy, Faculty of Science and Engineering, Åbo Akademi University, Finland
[h]Natural Resources Institute Finland (LUKE), Keminmaa, Finland
[i]Novia University of Applied Sciences, Ekenäs, Finland

Abstract

The elemental composition of otoliths provides historical information on migration and provenance of fish. Due to the complex structure of the otoliths, the depth from which the elemental information originates has to be considered. In this work, three analytical methods often used to assess otolith chemistry are compared. The information depths are calculated for μ-XRF and PIXE and measured for LA-ICP-MS. The information depth in PIXE depends on the energy of the incident particles and on the element to be analysed while in XRF it depends mostly on the element to be analysed as the energy of the incident X-rays usually is high enough to excite atoms at depths of several hundreds of micrometres. If we assume that the otolith is exposed to X-rays from a Rh-tube (20.16 keV) about 50 % of the detectable Sr(Kα) X-rays will be emitted from a depth ranging from 0 to 114 μm. In the case of PIXE with 3 MeV protons the corresponding range is 0 to 15 μm. The information depths in LA-ICP-MS were determined by measuring the depth of the laser-ablated craters or trenches that remained on the otolith surface. The depths measured with a scanning white light interferometer (SWLI) were found to be about 40 μm (spots) and 11 μm (trenches).

The correlation between strontium concentrations obtained by spot analysis of whitefish otoliths with PIXE and LA-ICP-MS was excellent (92%), although different spot sizes were used. A comparison of strontium concentration profiles measured with μ-XRF and LA-ICP-MS showed that the higher information depth of μ-XRF in combination with the 52 degree angle of the incident X-rays smoothens out the sharp edges seen in the LA-ICP-MS profiles. Otoliths from whitefish captured in the Baltic Sea (n=30) were analysed in this comparison of methods. Among these whitefish there are sea spawners, river spawners and stocked fish with different life history and different otolith chemistry.

Keywords: Otolith, elemental analysis, information depth, LA-ICP-MS, PIXE, XRF, whitefish, Baltic Sea

Corresponding author: Lill, Jan-Olof, Accelerator Laboratory, Turku PET Centre, Åbo Akademi University, Porthansg. 3, FI-20500 Turku, Finland, E-mail: jlill@abo.fi

1. Introduction

Otolith chemistry is a useful tool in the tracking of fish migration, in the discrimination of fish stocks and in the monitoring of aquatic environments. Otoliths are calcified structures found in otic sacs in the inner-ear of fishes. The inner ear is a paired structure of canals, ducts and sacs located in the cranium of the fish, functioning as an auditory and a vestibular system. In the otic sacs the otoliths are suspended in endolymph and fixed by a membrane over a sensory tissue [1].

The Osteichthyan fish have three pairs of otoliths, namely sagitta, lapillus and asteriscus of which sagitta is the largest and therefore most often used for age reading and elemental analysis. The sagitta is laterally flattened, and for most species, left-right symmetrical. Along the medial surface of the sagitta, a groove sulcus acusticus is located which allows contact to the sensory tissue [1]. The sagitta is made up of calcium carbonate (~96%), mainly as aragonite although vaterite sometimes is found, proteins (~3%), and other elements (~1%) [2].

The sagitta is built up three dimensionally starting from a primordium by biomineralization of calcium carbonate ($CaCO_3$) within a matrix of proteins on the otolith surface. The primordium retains a maternal signature as the egg is provisioned using nutrients derived from the mother and is often referred to as the mother tag [3]. The proportion of $CaCO_3$ and proteins incorporated into the otolith varies with season. During periods of fast growth i.e. summers, a higher proportion of $CaCO_3$ is incorporated into the otolith forming wide translucent zones while during periods of slower growth i.e. winters, less $CaCO_3$ and more proteins are incorporated forming thinner opaque zones commonly referred to as annuli [4]. The continual growth throughout the fish's life as well as the lack of resorption, even during periods of starvation, makes otoliths the preferred structure for age determination, especially in long-lived species [5].

During the biomineralization process, other elements are incorporated into the otolith as well, either as carbonates, as elements trapped in crystal defects or as elements bound to the proteinaceous matrix [2]. Divalent metal ions of comparable size and charge to Ca such as Sr^{2+} and $Ba^{2+,}$ can be incorporated through substitution for Ca in $CaCO_3$, or through co-precipitation as carbonates [2].

The rates of incorporation of elements such as Sr and Ba that are not under strict physiological regulation have been shown to reflect the availability in the ambient environment [e.g., 6]. Especially Sr, a proxy for salinity, has often been used to track migration over salinity gradients and to detect anadromy [5]. However other elements considered to be under physiological control can also be studied to infer aspects of the fish's life history. Magnesium (Mg), an element that is considered to be under physiological control [2] and therefore not likely to reflect the ambient environment has been studied to infer metabolic activity [7].

Particle Induced X-ray Emission (PIXE) and X-ray Fluorescence Spectrometry (XRF) analysis are non-destructive methods well suited for measuring strontium and zinc distributions or multi-elemental mapping of otoliths. The information depth in PIXE depends on the energy of the incident particles and on the element to be analysed, while in XRF it mostly depends on the element to be analysed. Laser Ablation Inductively Coupled Plasma

Mass Spectrometry (LA-ICP-MS) is sensitive enough to measure a wide variety of elements, but the calibration is demanding as it is carried out using multiple matrix-matched external standards containing the elements of interest combined with a single internal standard. The information depths in LA-ICP-MS can be determined by measuring the depth of the laser-ablated craters or trenches that remains on the otolith surface.

A general definition of the information depth in a solid specimen is the maximum depth, normal to the solid surface, from which useful signal information is obtained [8]. Bearing in mind that X-rays techniques suffer from an exponential attenuation law, it is convenient to define the information depth as the specimen thickness from which a specified percentage (for example 50% or 90%) of the detected signal originates.

In this study, we compare the information obtained by analysing whitefish otoliths with µ-XRF, PIXE and LA-ICP-MS. The whitefish (n=30) were captured in the Baltic Sea close to their spawning grounds [9]. Among these whitefish there are sea spawners, river spawners and stocked fish with different life history and different otolith chemistry.

2. Experimental

2.1. Preparation of whitefish otoliths

Prior to elemental analysis, a common preparation method is to embed the otolith in epoxy, sulcus side down, and polish the upward facing surface until the core is visible. The first annual growth ring is usually the largest, while the rest of the annuli are more densely spaced. The material within the first annual ring reveals the chemical environment during the first year of the fish. The shallow structure of the growth rings in the sagittal plane of otoliths prepared in this way may pose a risk for interference from the underlying growth rings, representing other parts of the life history. Furthermore, the depth of the first growth ring is in fact smaller beneath the core due to the shape of the sulcus acusticus.

Figure 1 shows a cross section of an otolith from a nine year old whitefish. The whole thickness of an unprepared otolith from a mature whitefish is about 1 mm and the width is about 4 mm. By analysing a transect on the polished otolith surface from the core towards the edge a historical record of the chemical environment of the fish is obtained. Although the first annual growth ring and the corresponding depth layer is clearly the largest, the layer thickness varies between 0.5 mm at most to about 0.2 mm near the sulcus that forms a ridge-like structure deforming the annual rings (Fig. 1).

2.2. Analytical methods

Two-dimensional element distribution maps of the polished otoliths were acquired using a M4 Tornado µ-XRF spectrometer. The spectrometer was equipped with an Rh X-ray tube and two silicon drift detectors manufactured by Bruker Nano. The diameter of X-ray beam was 20 µm and the sample chamber was evacuated to 20 mbar. The PIXE analysis of the polished otoliths was performed in air with a 3 MeV proton beam from the MGC-20 cyclotron [9]. The LA-ICP-MS analysis was performed at the Geological Survey of Finland (GTK) using a Nu AttoM SC-ICPMS (Nu Instruments Ltd., Wrexham, UK) and an Analyte 193 ArF laser-ablation system (Photon Machines, San Diego, USA). For the calibration and evaluation of the analysis the FEBS1 (certified otolith standard for trace metals, NRCC, Canada), NIST612 (synthetic silicate standard, NIST, USA), MACS-3 (synthetic silicate standard, USGS, USA) and CACB-1 (calcium carbonate standard, NRCC, Canada) certified reference materials were

used. In the LA-ICP-MS measurements of the otoliths, ^{43}Ca was used as an internal standard for quantification to increase the precision.

3. Results

3.1. Calculated information depths in µ-XRF

In XRF, the energy of the incident X-rays is usually high enough to excite atoms at depths of several hundreds of micrometres. The photon induced X-rays are also attenuated in the sample material on their way to the detector and the information depth will therefore not only depend on the energy of the incident radiation but primarily on the energy of the emitted X-rays. The absorption in the otolith was calculated using a weighted sum of mass attenuation coefficients for the main elements in the otolith. Exponential fits to X-ray mass attenuation coefficients from NIST were used in the calculations [10].

The information depth for X-ray based methods are presented as the depth range from which 50% or 90% of the detectable X-rays are emitted (Fig. 2). If we assume that the otolith is exposed to X-rays from a Rh-tube (20.16 keV), about 50 % of the detectable Sr(Kα) X-rays will be emitted from a depth range from 0 to 114 µm (Table 1). A matrix of $CaCO_3$ and a density of 2.93 g/cm^3 were used in the calculation [6]. In the mapping of strontium, it would be preferable to use the Sr(Lα) instead due to the lower energy and thereby much smaller depth range (0 to 2.6 µm) but preliminary test showed that the signal was too weak. Increasing the energy of the incident X-rays to 30 keV would increase the information depth further. However, the characteristic X-ray peaks will still dominate the X-ray spectrum emitted from the X-ray tube. No angular corrections have been made to the corrections above. In mapping with µ-XRF, the X-ray tube is located at a 52 degree angle and the detectors in angles of 45 degree to the sample surface. This arrangement decreases the information depth but also effects the 2D projection of structures beneath the surface (Fig. 3).

3.2. Calculated information depths in PIXE

The particle range limits the depth in ion beam techniques like PIXE. The stopping range of 3 MeV protons in otoliths is about 66 µm according to SRIM [11]. The same composition and density as earlier described were assumed. The K-shell ionization cross sections were obtained by fitting a polynomial function to the values of Chen and Crasemann [12]. The cross sections drop quit rapidly as the particle loses energy in the otolith matrix and the resulting information depth is no more than 15 µm (50% of the detectable Sr(Kα), see Table 1). The attenuation of the emitted strontium K X-rays from this shallow depth is almost negligible. In this case as well the absorption in the otolith was calculated using a weighted sum of mass attenuation coefficients obtained from exponential fits to X-ray mass attenuation coefficients from NIST [10].

The information depth in PIXE can be reduced by lowering the kinetic energy of the incident proton beam. Already at 2 MeV the information depth is only 8 µm (50% of the detectable Sr(Kα), see Table 1).

3.3. Measured depths of ablated trenches and craters in LA-ICP-MS

In LA-ICP-MS, the obtained concentrations are averages of the ablated volume. The ablation rate depends on the power and the wavelength of the laser, and to some extents also on the colour and refraction index of the sample. The trenches made by a 193 nm laser (2.5 J/cm^2, 10

Hz, 3 µm/s lateral speed on a polished whitefish otolith were measured to be 11 µm deep and 39 µm wide (Fig. 4 and Fig. 5). The single spots were measured to be somewhat deeper (40 µm), although the diameter of the spots was about 85 µm. The results agree with the rule of thumb that the ablation rate is 1 µm/s in calcium carbonate. The depth of the ablated trenches and craters were measured with the Scanning White Light Interferometry (SWLI) technique (Fig. 5). The instrument used was a customized scanning white light interferometer [13], with a total system magnification of 6.3x. The accuracy of the measurements in the z-direction was ± 15 nm. Image data-analysis and visualization were performed using MountainsMap Imaging Topography 7.2-software (Digital Surf, Avencon, France). As the method is based on the recombination of reflected white light from the sample surface and of reflected white light from a reference plane in the microscope objective, plane surfaces are the ideal situation when imaging and mapping the topography of a sample with SWLI technique. In this case, rough surfaces at the edges of the craters and trenches are imaged by the interferometer (Fig. 4). The roughness of these edges is not an artefact but originates from otolith material splattered during the LA-ICP-MS analysis.

3.4. Comparison of spot analyses with PIXE and LA-ICP-MS

In population studies it is of great importance to include a significant amount of fish in the study. Spot analysis is faster than whole transects and is therefore more efficient. The location of the spot on the otolith is crucial but the choice of spot size (width and depth) should be carefully considered to avoid interference from the mother tag and the sulcus. However, in provenance studies with a spot size more than 100 µm, the effect from the mother tag seems to vanish. The correlation between strontium concentration measured in the otolith core with PIXE (0.5 mm spot size, 90% from 0-37 µm) and LA-ICP-MS (85 µm spot size, 100% from 0-40 µm) was found to be strong (Fig. 6). The laser-ablated spots were located about 200 µm away from the core to avoid interference from the mother tag.

3.5 Comparison of strontium concentration profiles with µ-XRF and LA-ICP-MS

A comparison of the strontium concentration profiles measured with µ-XRF and LA-ICP-MS showed that the larger information depths of µ-XRF in combination with the 52 degree angle of the incident X-ray beam smoothens out the sharp edges seen in the LA-ICP-MS profiles (Fig.7). The semiquantitative µ-XRF profile has been normalized to the LA-ICP-MS profile to assist the reader. The µ-XRF profile was constructed of five adjacent spots extracted from previously measured maps resulting in a 100 µm wide profile compared to the 35 µm wide trench ablated by the laser.

4. Conclusions

Due to the variation in thickness within the annual growth rings of the otoliths, especially close to the core where the sulcus forms a ridge-like structure, the information depths of the analytical methods used have to be carefully considered in the interpretation of the results. In our case, the depth from the polished otolith surface to annual rings deformed by the sulcus ridge is less than 100 µm. Almost 50% of the detectable strontium X-rays in the µ-XRF maps in this region exceeds this depth making the sulcus visible in the 2D maps. In the case of strontium the information depths of PIXE (3 MeV) and LA-ICP-MS are comparable and the results of spot analysis of 30 whitefish otoliths correlate well. The lower detection limits obtained by LA-ICP-MS are, however, a great advantage as interesting elements such as barium, manganese and magnesium can be measured in the otoliths.

Acknowledgement

The help from Jan Gustafsson, Staffan Dahlström and Linnea Nordblom at Åbo Akademi University, and from Birthe Wistbacka, at the Norra svenska fiskedistriktet in Ostrobothnia, is gratefully acknowledged.

References

[1] J. Panfili, H. de Pontual, H. Troadec, and P. J. Wright (Eds.), Manual of fish sclerochronology (Ifremer, Brest, 2002) 464 p.

[2] S. Campana, Chemistry and composition of fish otoliths: pathways, mechanisms and applications, Mar. Ecol. Prog. Ser. 188 (1999) 263-297.

[3] J.C. Hegg, B.P. Kennedy, P. Chittaro, What did you say about my mother? The complexities of maternally derived chemical signatures in otoliths, Canadian Journal of Fisheries and Aquatic Sciences, 76 (2019) 81-94.

[4] S. VanderKooy (Ed), A Practical Handbook for Determining the Ages of Gulf of Mexico Fishes. Second Edition, Gulf States Marine Fisheries Commission Publication Number 167, 2009.

[5] S. E. Campana and S. R. Thorrold, Otoliths, increments, and elements: keys to a comprehensive understanding of fish populations? Can. J. Fish. Aquat. Sci. 58 (2001) 30–38

[6] G. Bath, S. Thorrold, C. Jones, S. Campana, J. McLaren, and J. Lam, Strontium and barium uptake in aragonitic otoliths of marine fish, Geochim. Cosmochim. Acta 64 (2000) 1705-1714.

[7] K. E. Limburg, M. J. Wuenschel, K. Hüssy, Y. Heimbrand and M. Samson,: Making the Otolith Magnesium Chemical Calendar-Clock Tick: Plausible Mechanism and Empirical Evidence, Reviews in Fisheries Science & Aquaculture, 26 (2018), 479-493.

[8] J. Rubio-Zuazoa, and G. R. Castro, Information depth determination for hard X-ray photoelectron spectroscopy up to 15 keV photoelectron kinetic energy, Surf. Interface Anal., 40 (2008) 1438–1443.

[9] J-O. Lill, V. Finnäs, J.M.K. Slotte, E. Jokikokko, Y. Heimbrand, H. Hägerstrand, Provenance of whitefish in the Gulf of Bothnia, Baltic Sea, determined by elemental analysis of otolith cores, Nucl. Instr. Meth. B 417 (2018) 86-90.

[10] J. H. Hubbell and S. M. Seltzer, Tables of X-Ray Mass Attenuation Coefficients and Mass Energy-Absorption Coefficients from 1 keV to 20 MeV for Elements Z = 1 to 92 and 48 Additional Substances of Dosimetric Interest, NIST Standard Reference Database 126 , Accessed 09.04.2019 <https://www.nist.gov/pml/x-ray-mass-attenuation-coefficients>.

[11] J. F. Ziegler, M. D. Ziegler, J. P. Biersack, SRIM - The Stopping and Range of Ions in Matter, Accessed 09.04.2019 <http://www.srim.org/>.

[12] M.H. Chen and B. Crasemann, Relativistic cross sections for atomic K- and L-shell ionization by protons, calculated from a Dirac-Hartree-Slater model, Atomic Data and Nuclear Data Tables, 33 (1985) 217-233.

[13] N. Sandler, I. Kassamakov, H. Ehlers, N. Genina, T. Ylitalo and E. Haeggstrom, Rapid interferometric imaging of printed drug laden multilayer structures, Sci. Rep. 4, 4020 (2014) 1-5.

Tables

Table 1. Strontium information depths in otoliths calculated for µ-XRF and PIXE and measured from the depths of trenches and craters for LA-ICP-MS. Information depths are reported as the thickness in µm from the surface from which a specified percentage of the detected signal originates. The Sr(Lα) signal was unfortunately too weak to be useful in PIXE and µ-XRF. No geometrical corrections were made.

Analytical method	Sr(Kα)		Sr(Lα)	
	50 %	90 %	50 %	90 %
µ-XRF (Rh tube, 20.16 keV)	114	377	2.6	8.7
µ-XRF (30 kV)	148	491	2.6	8.7
PIXE (3 MeV)	15	37		
PIXE (2 MeV)	8	22		
LA-ICP-MS (spot 85 µm)	20	36	20	36
LA-ICP-MS (trench 39 µm)	6	10	6	10

Figure Captions

Fig. 1. Cross section of whitefish otolith. The width is ~4.0 mm and the thickness ~1.1 mm. The sulcus is seen on the lower part of the otolith. The upper part is normally removed by grinding and polishing until the core region is visible.

Fig. 2. Transmission of Sr(Kα) and Sr(Lα) induced by Rh(Kα) in an otolith as a function of depth.

Fig 3. Strontium concentration maps of otoliths measured with µ-XRF. The spot size was 20 µm. The otolith to the right is from a seven years old stocked whitefish (H7, [9]). A M4 Tornado µ-XRF spectrometer was used for the mapping.

Fig. 4. Microscope picture of a polished whitefish otolith (H7 in Fig. 3) that has been subjected to a laser beam. The diameter of the three spots is 85 µm. The width of the ablated trench is 39 µm and the length about 2 mm.

Fig. 5. A 3D projection of the ablated trench that can be seen in figure 4. The surface structure was measured with a scanning white light interferometer (SWLI).

Fig. 6. Strontium concentrations in the core region of 30 whitefish otoliths measured with PIXE and LA-ICP-MS. The correlation was 0.92 although the spot size of PIXE was about 0.5 mm [9] and the spot size of LA-ICP-MS was 85 µm (Fig. 5). The information depth was of the same order (Table 1).

Fig. 7 Strontium concentrations obtained with LA-ICP-MS from the transect on the polished whitefish otolith in Fig. 4 (H7). The width of the ablated trench was 39 µm and the depth 11 µm. The semi quantitative profile obtained with µ-XRF has a somewhat different shape as the X-ray tube was located at a 52 degree angle to sample surface. All concentrations are in µg/g of dry weight.

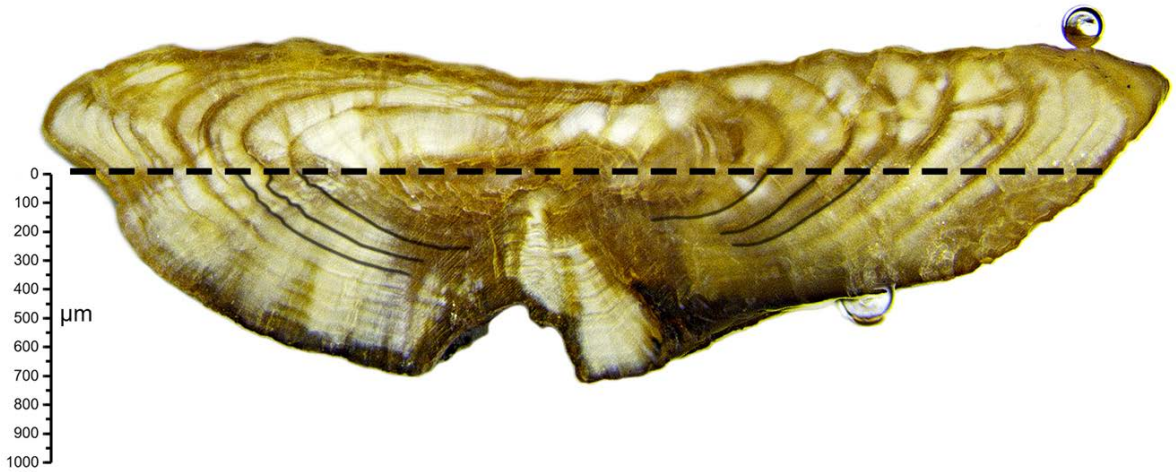
0
100
200
300
400
500
600
700
800
900
1000
µm

Fig. 1.

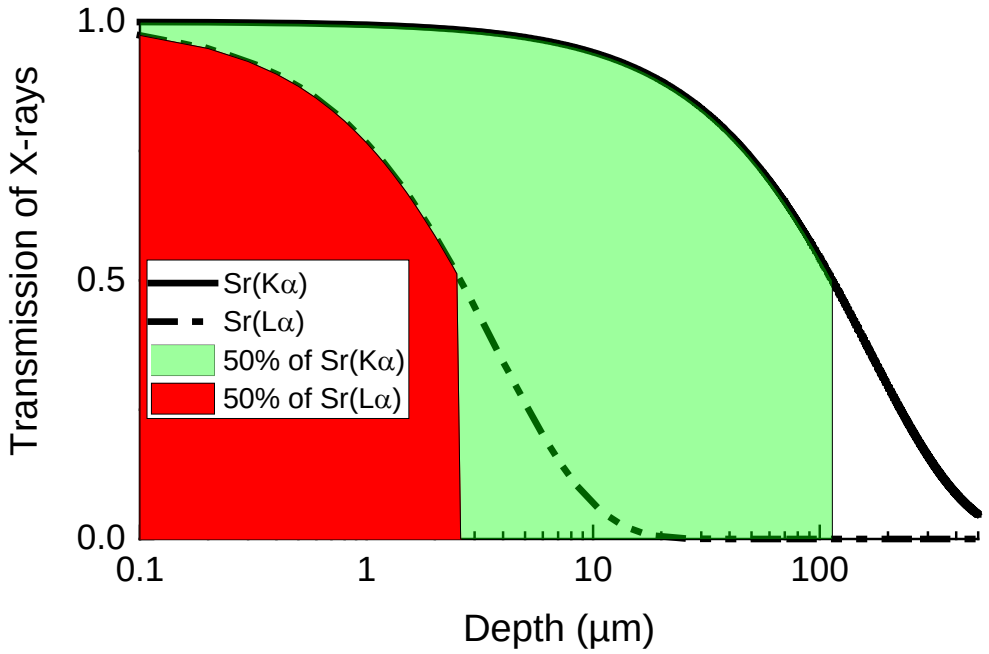
1.0
0.5
0.0
Transmission of X-rays
Sr(Kα)
Sr(Lα)
50% of Sr(Kα)
50% of Sr(Lα)
0.1
1
10
100
Depth (µm)

Fig. 2.

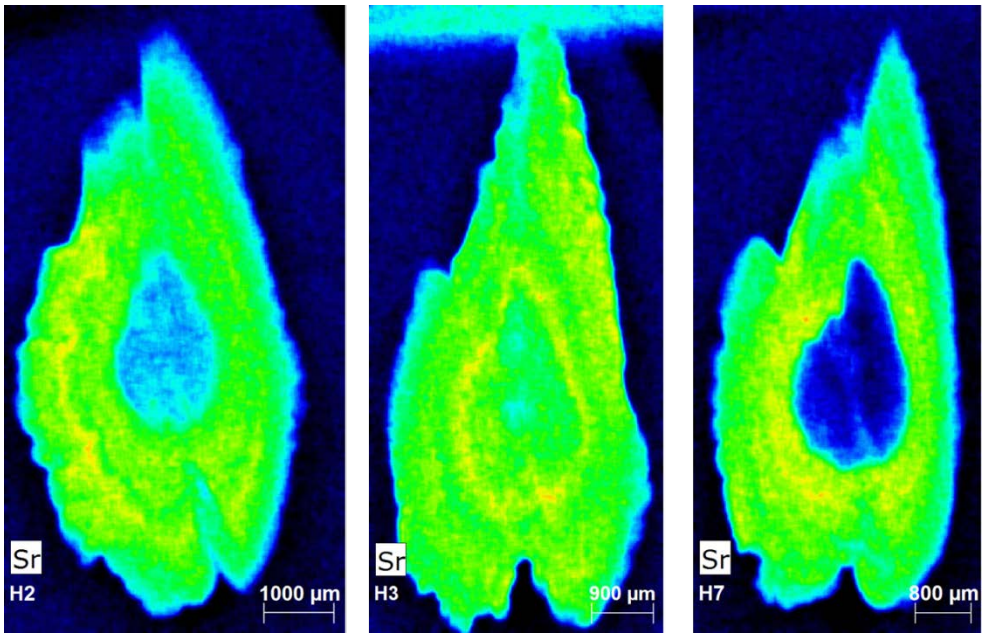

Fig. 3.

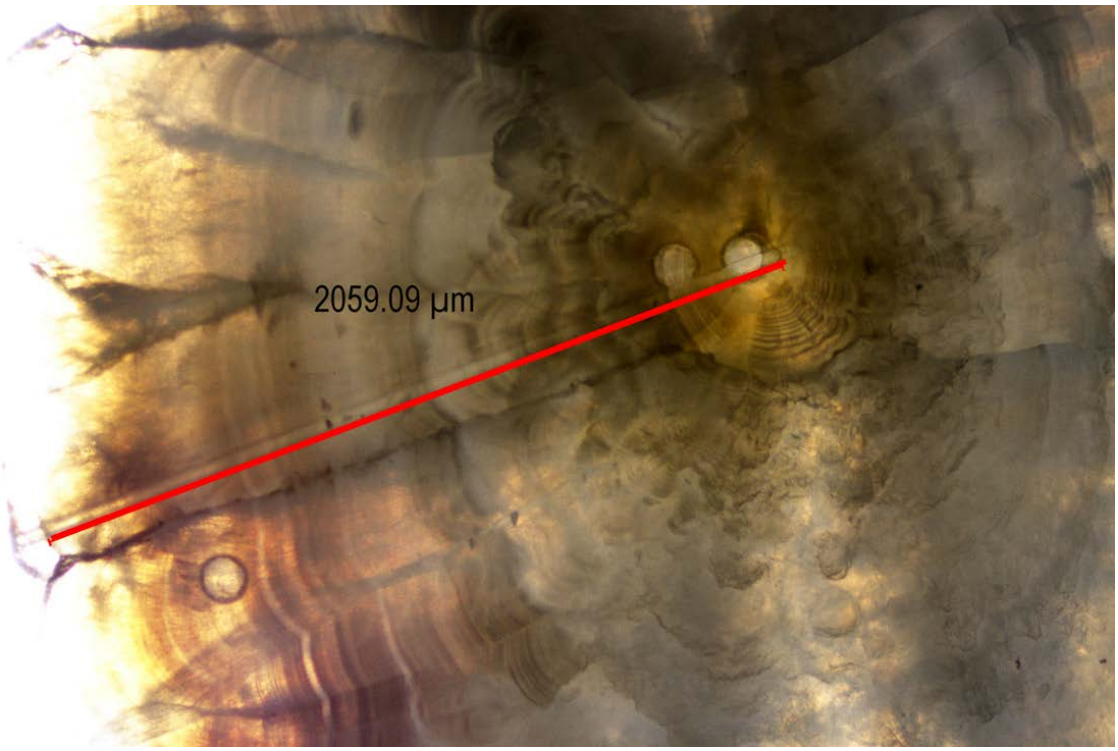

Fig. 4.

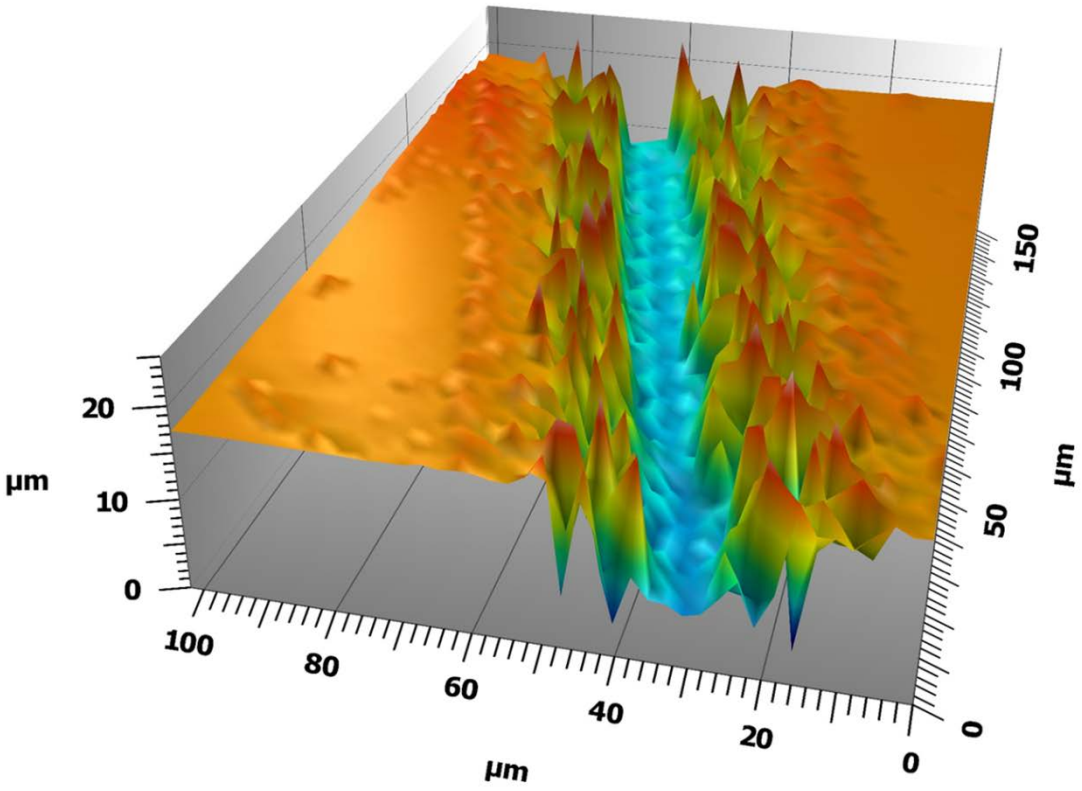
µm
20
10
0
100
80
60
40
20
0
µm
0
50
100
150
µm

Fig. 5.

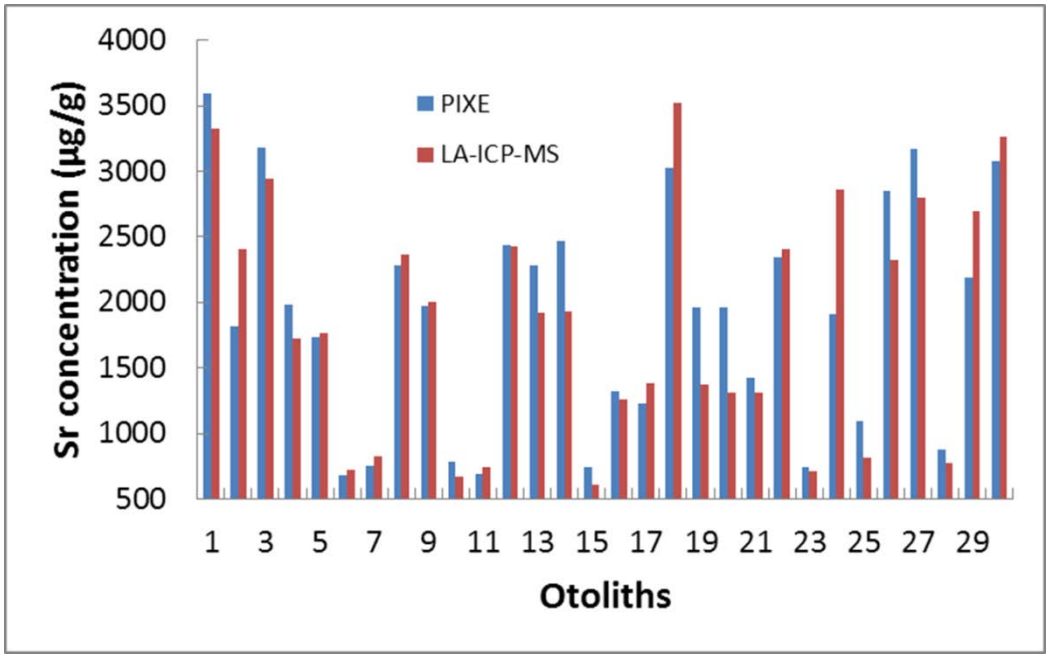
Sr concentration (µg/g)
4000
3500
3000
2500
2000
1500
1000
500
PIXE
LA-ICP-MS
1 3 5 7 9 11 13 15 17 19 21 23 25 27 29
Otoliths

Fig. 6.

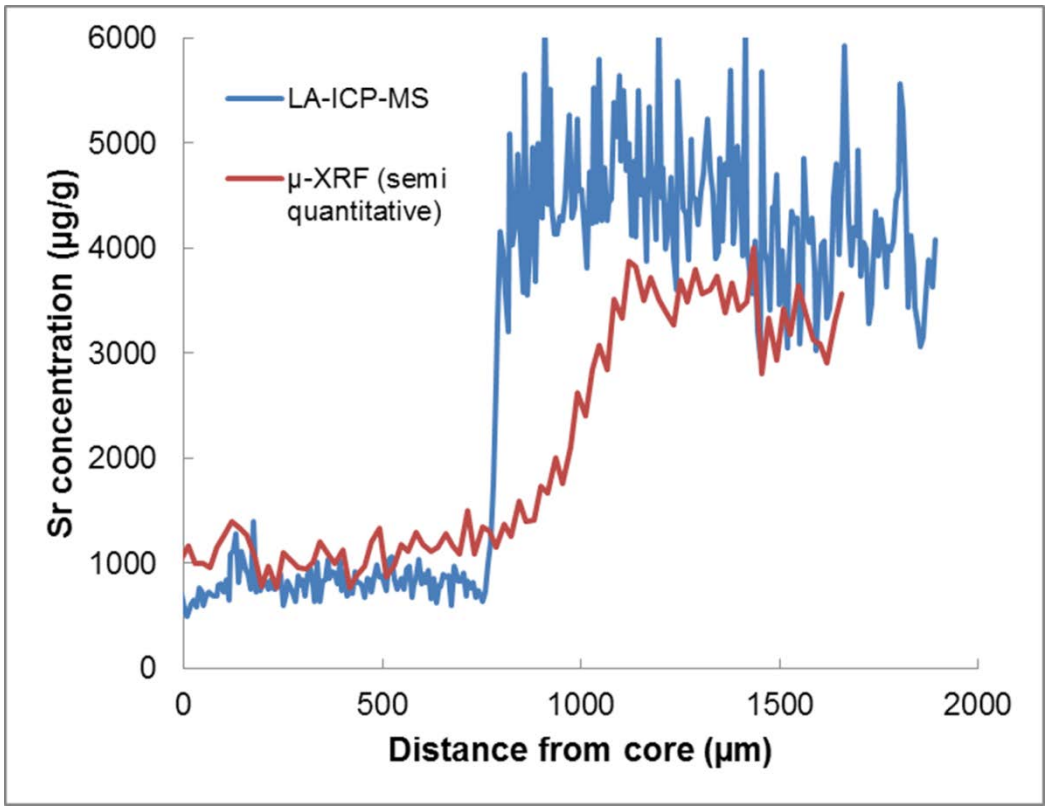
6000
5000
4000
3000
2000
1000
0
Sr concentration (µg/g)
LA-ICP-MS
µ-XRF (semi quantitative)
0
500
1000
1500
2000
Distance from core (µm)

Fig. 7.